Multiple noise-like pulsing of a figure-eight fibre laser

2014 Laser Phys. 24 015103

(http://iopscience.iop.org/1555-6611/24/1/015103)

IOP Publishing | Astro Ltd Laser Physics

Laser Phys. **24** (2014) 015103 (9pp) doi:10.1088/1054-660X/24/1/015103

Multiple noise-like pulsing of a figure-eight fibre laser

O Pottiez[1], B Ibarra-Escamilla[2], E A Kuzin[2], J C Hernández-García[2], A González-García[2] and M Durán-Sánchez[3]

[1] Centro de Investigaciones en Óptica (CIO), Loma del Bosque 115, Colonia Lomas del Campestre, León, Guanajuato 37150, Mexico
[2] Instituto Nacional de Astrofísica, Óptica y Electrónica (INAOE), L E Erro 1, Santa Maria Tonantzintla, Puebla 72824, Mexico
[3] Mecatrónica, Universidad Tecnológica de Puebla, Antiguo Camino a la Resurrección 1002-A Parque Industrial, Puebla 72300, Mexico

E-mail: pottiez@cio.mx

Received 14 October 2013
Accepted for publication 20 November 2013
Published 10 December 2013

Abstract

In this work we study multiple noise-like pulse generation in a 320 m long passively mode-locked erbium-doped figure-eight fibre laser in the normal net dispersion regime. The nonlinear optical loop mirror (NOLM) that is used as a mode locker operates through polarization asymmetry, which allows us to control its switching power by birefringence adjustments at the NOLM input, using a half-wave retarder (HWR). Over some range of the HWR orientation, a single noise-like pulse is observed in the cavity. Its peak power is adjustable as it remains clamped to the variable switching power, and its duration varies inversely between ∼5 and ∼22 ps. Beyond the HWR position, corresponding to the longest duration, the pulse splits into several noise-like pulses. These multiple pulses usually present a walkoff, however they can be synchronized through slight birefringence adjustments, although they are not evenly spaced in time. Up to 12 simultaneous noise-like pulses were observed experimentally, with a duration of ∼2 ns. Multiple pulsing and synchronization of the pulses are interpreted in terms of mechanisms of interaction between pulses. Multiple pulsing appears to be indirectly related to the peak power limiting effect of the NOLM.

Keywords: fibre lasers, passive mode locking, noise-like pulses, multiple pulsing

1. Introduction

Passively mode-locked fibre lasers are attractive low-cost sources of ultrashort pulses that have been extensively investigated in the past. Recently, as high-power pump diodes have become readily available, there has been a renewed interest in these fibre lasers for the generation of high-energy pulses [1–3], which are useful for applications like supercontinuum generation and sensing, among others. Unfortunately, it was soon realized that the highest achievable pulse energy is limited by the onset of multiple pulsing. In the anomalous dispersion regime, as pump power is increased, multiple solitons tend to appear in the regime, all sharing the same properties (soliton quantization) [4]. Recently, heavily multipulse regimes have been observed, in which several tens or hundreds of pulses coexist and interact in the cavity in various ways [5, 6], resulting in the emergence of a wide variety of regimes [7] which differ in different respects: the pattern may remain stable over successive round-trips or not, the pulses may be regularly spaced or randomly distributed, and they may be either distributed over the whole cavity length or condensed into a bunch whose duration is shorter than the cavity round-trip time. A particularly interesting regime is established when a large number of equally spaced pulses extends over the whole cavity length: high-order harmonic mode locking is then achieved, yielding stable pulse trains with repetition rates up to several GHz, which are attractive, in particular, for high-speed transmission applications [5, 8–11]. In the normal dispersion regime, the formation of highly chirped pulses with very long durations

allows for much higher pulse energy [12–15], and in some cases single-pulse operation up to an arbitrarily large energy is even possible [16]. In spite of this, multiple pulsing is still likely to occur in this regime [16–18].

The mechanisms leading to multiple pulsing in passively mode-locked fibre lasers have been studied in previous works. In [19], multiple soliton formation is explained by the peak power limiting effect of the saturable absorber. In other configurations [18, 20, 21], multiple pulsing occurs when, due to its large bandwidth, a single pulse suffers high losses through the bandwidth-limited gain medium. The latter argument can be invoked when the pulse bandwidth becomes comparable with the optical gain bandwidth. In many cases however, multiple pulsing appears while the optical spectrum is still much narrower than the gain bandwidth.

A particular category of pulses, the so-called noise-like pulses, were observed recently in both anomalous [22–30] and normal [31–33] dispersion regimes and are now attracting a growing interest due to their high energy and wide spectrum, in some cases extending beyond 100 nm [29]. Fundamentally, a noise-like pulse is a large, ∼ns collection of thousands of ultrashort (sub-ps) pulses with randomly varying amplitudes and durations that are packed together. Therefore, in a sense, the formation of a noise-like pulse in a laser cavity constitutes a particular kind of multiple pulsing phenomenon. Although there is no consensus in the literature on the physical mechanisms involved in their formation, the peak power limiting effect of the saturable absorber has been invoked [31]. Typically the sub-pulses remain stuck together, so that a single noise-like pulse circulates in the cavity. If pump power is increased, the number of sub-pulses, and thus the energy of the bunch, increases proportionally [24]. However, a few cases of dual noise-like pulsing in passively mode-locked fibre lasers have been reported [23, 30]. For most applications, multiple pulsing is not desired, as it sets an upper limit to the pulse energy and bandwidth, which are critical for applications such as supercontinuum generation and sensing [34, 25, 35].

An important category of passively mode-locked fibre lasers is the so-called figure-eight laser scheme [36]. In this architecture, the role of saturable absorber, which is responsible for pulse formation and shortening, is played by a nonlinear optical loop mirror (NOLM) [37], or alternatively by a nonlinear amplifying loop mirror (NALM) [38], which is inserted into a fibre ring structure. The nonlinear switching characteristic of a NOLM or NALM is due to the Kerr-induced nonlinear phase difference between the beams that counter-propagate in the loop, and takes the form of a sinusoidal function of input power. In conventional schemes, this nonlinear phase difference is due to a power imbalance between the two beams. A drawback of conventional NOLMs, however, is the limited flexibility of their switching characteristic, whose properties (in particular switching power and dynamic range) are usually fixed by construction. Therefore, the NOLM should be carefully designed for proper mode locking operation.

Aside from conventional, power-asymmetric NOLM schemes, an alternative design was proposed, which relies on a polarization imbalance [39]. As a 50/50 coupler is used, the device is power-symmetric, and polarization asymmetry is created by a quarter-wave retarder (QWR) in the loop. Polarization-dependent nonlinear phase shift (or equivalently nonlinear polarization rotation, NPR) then provides switching. The fibre is twisted to mitigate the effects of residual birefringence and to induce optical activity, ensuring a nearly isotropic behaviour, so that light ellipticity is conserved during propagation [40]. As a consequence, the nonlinear phase shift difference does not average out but instead accumulates along the loop. As the NOLM operation depends on the polarization of light at its input and inside the loop, the switching characteristic can be readily adjusted through the orientation of wave retarders: the dynamic range and low-power transmission are controlled by the QWR, and the switching power by a half-wave retarder (HWR) inserted at the NOLM input [41, 42]. Noise-like pulses with adjustable characteristics were successfully generated by a figure-eight laser including such a polarization-imbalanced NOLM [28], and these pulses proved to be useful for supercontinuum generation in a piece of standard fibre [35].

In this work we study noise-like pulse generation in a long figure-eight fibre laser operating in the normal dispersion regime and including a polarization-imbalanced NOLM. We report in particular what we believe is the first experimental demonstration of multiple (>2) noise-like pulsing in a fibre laser and show that this operation is related to the power limiting effect of the saturable absorber.

2. Experimental setup

The experimental setup is presented in figure 1. The total length of the laser is 320 m. It includes a ring section (left side of the figure) and a polarization-imbalanced NOLM (right). The ring cavity includes a 200 m piece of dispersion-compensating (DCF) fibre ($D = -38$ ps nm^{-1} km^{-1}), which imposes the laser operation in the average normal dispersion regime. The ring also includes two sections of erbium-doped fibres (3 m EDF1 and 2 m EDF2) with 30 dB m^{-1} absorption at 1530 nm, which are pumped at 980 nm through WDM couplers. The pump powers into EDF1 and EDF2 are ∼300 mW and ∼200 mW respectively. A polarizer ensures linear polarization at the NOLM input, whose angle ψ can be adjusted by a HWR. A polarization controller (PC) made of two retarder plates is used to maximize the power through the polarizer. An optical isolator ensures unidirectional laser operation. Two output couplers with 10% output coupling are used as the laser output ports.

The NOLM is formed by a 50/50 coupler and a 100 m loop of low-birefringence fibre. The fibre is twisted at a ratio of 5 turns m^{-1}, which ensures that light ellipticity is maintained during propagation [40]. A QWR is inserted to break the polarization symmetry: the clockwise beam remains linearly polarized in the loop, however, the polarization of the counter-clockwise beam is turned elliptic by the QWR, the value of ellipticity depending on the angle ψ of input polarization with respect to the QWR. The fibre loop has an anomalous dispersion of ∼17 ps nm^{-1} km^{-1} and a nonlinear coefficient $\gamma = 1.5$ W^{-1} km^{-1}. With these parameters, the

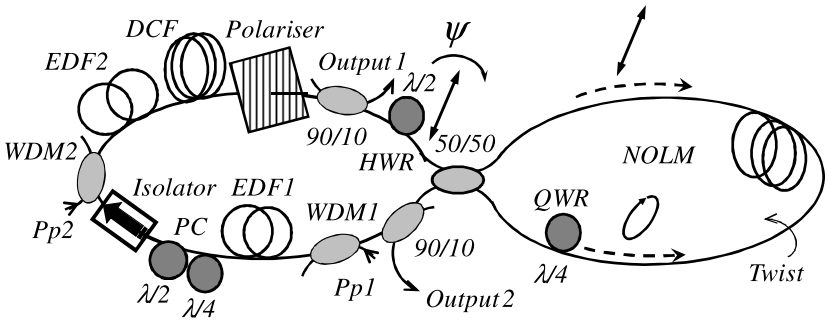

Figure 1. Scheme of the figure-eight laser under study.

minimum continuous-wave (CW) switching power of the NOLM is $P_\pi = 6\pi/\gamma L \approx 125$ W [41]. An important aspect of the NOLM architecture is that, by adjusting the angle ψ of the linear input polarization the NOLM switching power can be varied from this minimal value theoretically to infinity [41, 42]. On the other hand, the QWR angle controls the value of low-power transmission, which should be small for the pulsed operation regime, although not zero as some leakage is required to allow lasing to initiate [36].

3. Experimental results

For most orientations of the wave retarders, CW operation is spontaneously obtained at maximal pump power. In some of these cases, a mechanical stimulation (a kick) yields stable mode locking. Besides, some positions can also be found where mode locking starts spontaneously. The highest output power is observed at output 1, reaching up to ∼5 mW. Once mode locking is achieved, the characteristics of the generated pulse train can be widely varied by varying the orientation of the HWR over a given range, beyond which mode locking is lost, and is not recovered even after further mechanical stimulation.

One end of this HWR range corresponds to fundamental mode locking in which a single, high-power pulse circulates in the cavity. The 200 MHz scope trace (figure 2(a)) shows that the pulse train period is 1.6 μs (repetition rate = 625 kHz), corresponding to one round-trip time in the 320 m cavity. The solid line in figure 3(a) shows the pulse autocorrelation, which displays a double-scaled structure with a narrow (∼1 ps) peak riding a wide pedestal that extends beyond the 200 ps measurement window of the autocorrelator. The peak-to-pedestal level ratio is approximately 2:1. The pulse is also measured in the time domain using a 25 GHz photodetector and a 50 GHz sampling scope (figure 3(b), solid). This measurement shows that the average pulse envelope is nearly rectangular, with a duration of ∼5 ns. Finally, the pulse presents a wide and smooth optical spectrum, with a 3 dB bandwidth of 15 nm, as shown by a solid line in figure 3(c). The slight asymmetry of this spectrum and its peak wavelength shift to ∼1570 nm denote the presence of a Raman self-frequency shift in the cavity. All these measurements are the typical signature of noise-like pulses [22–33]. The duration of the narrow peak in the autocorrelation trace scales as the average duration of the sub-pulses that form the inner structure of the noise-like waveform. As the total duration of the bunch is 5 ns, it contains several thousands of ps and sub-ps pulses. These measurements also allowed us to estimate the pulse energy to ∼4 nJ.

It is important to note that the smoothness of the curves displayed in figures 3(b) and (c) is not an intrinsic property of noise-like pulses, but derives from the extreme variability of the sub-pulses in the bunch, together with the strong averaging performed during these measurements. Indeed, although the global properties of the noise-like pulses (total duration, average peak power, energy) remain constant in time, their inner structure varies strongly over successive round-trips. In the measurements obtained through averaging over a large number of pulses, the spiky details of the individual pulses average out, yielding very smooth curves [32].

If the HWR angle is now varied in the appropriate direction, the pulse progressively widens temporally whereas its duration increases (figure 2(b)). In the spectral domain, this evolution is accompanied by a reduction of the bandwidth. Dashed lines in figure 3 illustrate the final stage of this evolution, when the pulse reaches a maximal duration of ∼22 ns. At this point, the bandwidth has decreased down to ∼5 nm. In contrast, the autocorrelation is not significantly different from the previous case. In particular, the width of the coherence peak remains unchanged. The pulse energy is also roughly the same, reaching a value of ∼5 nJ.

When the HWR is further rotated, the wide single pulse starts to split into several pulses (figure 2(c)). Although in most cases the multiple pulses are not synchronized, leading to an unstable behaviour on the scope, slight adjustments of the wave retarders allow us to eliminate the walkoff, yielding stable multiple pulse patterns. Stable generation of two, three, four, five (figure 2(d)), ... and up to 12 nearly identical pulses (figure 2(e)) was successively observed, with decreasing values of peak power (compare figures 2(d) and (e)). Multiple pulse patterns remain stable for several minutes at least. The pulse spacing is typically not uniform, although when the number of pulses is large several pulses tend to appear with a constant separation of ∼20 ns. The dotted curves in figure 3 are measurements taken for 12 pulses. The pulses display a duration of ∼2 ns. The optical spectrum,

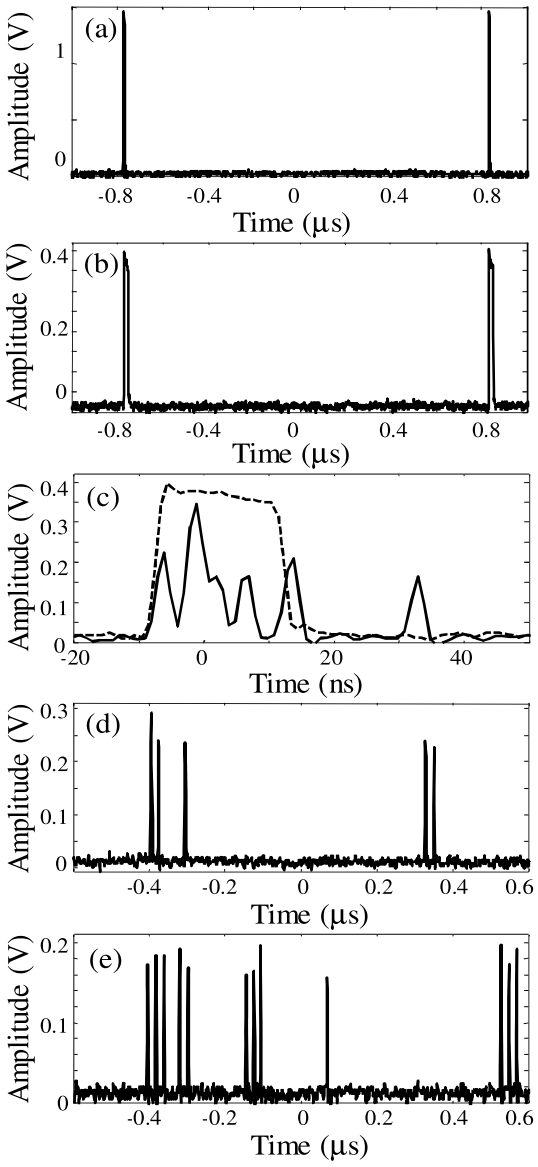

Figure 2. Scope traces of the pulses obtained for different HWR settings: (a) high-peak-power, 5 ns single pulse; (b) low-peak-power, 22 ns single pulse; (c) pulse breaking; (d) five and (e) 12 2 ns stable pulses. The dashed line in (c) reproduces the single pulse profile of (b) for comparison.

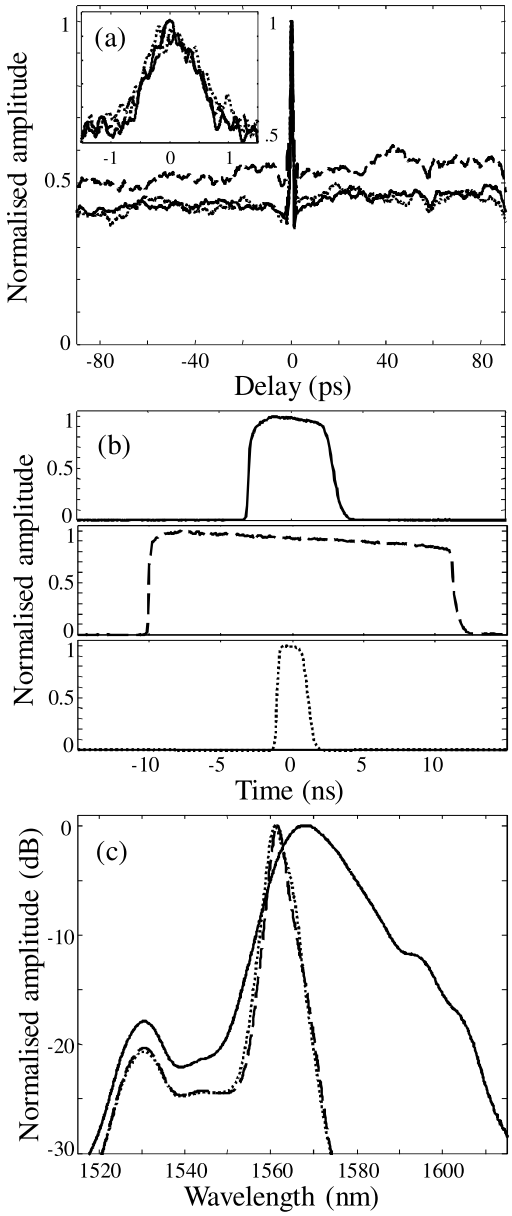

Figure 3. (a) Autocorrelation (the inset shows a close-up on the central spur), (b) sampling scope traces and (c) optical spectra of the pulses obtained for three different HWR settings, corresponding to the generation of a high-peak-power, 5 ns single pulse (solid), a low-peak-power, 22 ns single pulse (dashed) and 12 synchronized 2 ns pulses (dotted).

smooth and with a ∼4.5 nm bandwidth, is very similar to that of the single pulse just before breaking. The autocorrelation again displays a double-scaled structure, and does not present any significant variation with respect to the previous cases. These measurements confirm the noise-like nature of the multiple pulses. The total energy of the pulses is estimated to ∼2–3 nJ, and is roughly independent of the number of pulses.

Finally, for a few adjustments of the wave retarders, a distinct pulse regime is observed, in which the spectrum widens dramatically, yielding a 3 dB bandwidth as large as ∼50 nm and a Raman-induced peak wavelength shift to almost 1590 nm (figure 4(a)). In this regime, the 200 MHz scope displays a single pulse per round-trip whose amplitude and duration are similar to the case of the high-peak-power single pulse described previously (figure 2(a) and solid lines in figure 3). On the sampling scope however, a more complex inner structure consisting of three and up to four peaks appears, with the same peak power, a duration of ∼0.8 ns each and a uniform separation of ∼1.4 ns (figure 4(b)). These pulses present some degree of overlap as the power level between them does not reach zero. The double-scaled structure of the autocorrelation trace (figure 4(c)), together with the wide and smooth optical spectrum, confirms the noise-like nature of the quadruple pulses. In this case however, the width of the central spur is ∼200 fs, i.e. about five times shorter than in the previous regimes. This is consistent with the larger bandwidth observed in the spectral domain. Another

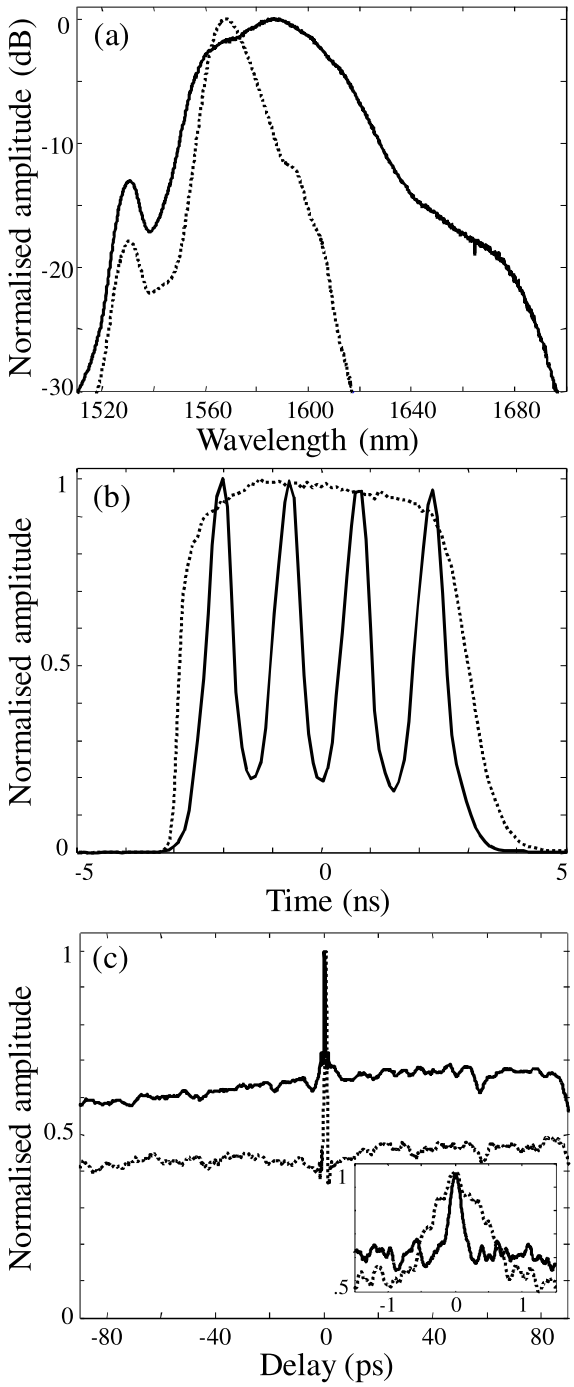

Figure 4. Optical spectrum (a), sampling scope trace (b) and autocorrelation (c) of the quadruple pulse (solid). The curves corresponding to the high-peak-power single pulse are also shown for comparison (dotted).

noticeable difference with respect to the previous regimes is the background level of the autocorrelation trace, which is now significantly above 0.5.

4. Numerical study and discussion

The dependence of the temporal and spectral properties of single noise-like pulses on the orientation of the HWR in a similar scheme (although in that case the laser was operating in the anomalous dispersion regime) was previously observed and reported in [28]. This mechanism can be summarized as follows. As mentioned above, the HWR angle controls the value of the NOLM switching power, to which the pulse peak power roughly adjusts as it corresponds to maximal NOLM transmission and thus minimal cavity loss. Referring to noise-like pulses, which are complex collections of sub-pulses with randomly varying amplitudes, peak power has to be understood in an average sense, however even in this case peak power clamping to the NOLM switching power actually takes place, as attested by the flat top of the pulse envelopes shown in figure 3(b). If switching power is increased, the peak power adjusts itself and grows. At a given pump power, the pulse energy is roughly constant, so that this peak power increase is associated with a reduction of pulse duration (i.e. reduction of the number of sub-pulses) and spectral widening, which is due basically to enhanced Kerr nonlinearity and Raman self-frequency shift at higher peak power. Conversely, if switching power decreases, peak power is reduced and the pulse widens temporally (more sub-pulses in the bunch). In the spectral domain, lower peak power also means weaker nonlinear effects and thus narrower bandwidth. In the anomalous dispersion regime, due to the soliton effect, higher peak power is also associated with a shorter duration of the sub-pulses, so that the width of the coherence peak in the autocorrelation measurement varies with HWR adjustment. In the present case however, in the normal net dispersion regime, the soliton effect is not believed to play a significant role in pulse formation; the pulses are strongly chirped and this inverse relation between peak power and duration no longer applies. The inset in figure 3(a) indicates that, on average, the duration of the sub-pulses is relatively large and is independent of the HWR position.

Because by nature a noise-like pulse consists of several thousands of ultrashort pulses, it is not submitted to the energy quantization that affects conventional pulses [4], so that in general a single noise-like pulse is present in the cavity. Under an increase in pump power [24] or, like in this case, when the saturation power (and thus the peak power) is reduced, the noise-like pulse naturally responds by increasing its duration, which means an increase in the number of sub-pulses in the packet, and one could believe that there is no upper limit to this widening. Our experimental results contradict this conclusion, however, as it turns out that beyond a certain upper duration limit (∼20 ns in our experiment), the pulse splits into several noise-like pulses.

To get further insight into the mechanisms involved in multiple noise-like pulse regimes, a numerical study was carried out. The laser scheme considered for numerical simulations is very similar to the scheme of figure 1 and uses the same fibre parameters, but with a few differences. First, both the lengths of the NOLM and of the DCF were reduced to 50 m in the model in order to save computational time. Besides, for simplicity only one 5 m section of erbium-doped fibre was modelled, and a parabolic approximation was used for the gain bandwidth. Finally, linear birefringence was neglected and the polarizer + HWR combination at the

NOLM input was replaced by a rotatable polarizer in the model. The QWR in the NOLM was oriented in order to get ~10% low-power NOLM transmission, a small yet non-zero value allowing the initial growth of laser oscillation [36]. Propagation in the laser cavity was modelled using a pair of nonlinear Schrödinger equations, which in the circular $[C^+; C^-]$ base can be written as

$$\begin{aligned}
\frac{\partial C^+}{\partial z} &= -\frac{\Delta\beta_1}{2}\frac{\partial C^+}{\partial t} - \mathrm{j}\frac{\beta_2}{2}\frac{\partial^2 C^+}{\partial t^2} + \frac{\beta_3}{6}\frac{\partial^3 C^+}{\partial t^3} \\
&\quad + \frac{g}{2}C^+ + \frac{1}{L_\mathrm{a}\Omega_\mathrm{a}^2}\frac{\partial^2 C^+}{\partial t^2} \\
&\quad + \frac{2\mathrm{j}\gamma}{3}(|C^+|^2 + 2|C^-|^2)C^+ \\
&\quad - \mathrm{j}\gamma T_\mathrm{R}\left[\frac{1+\alpha}{2}\frac{\partial}{\partial t}(|C^+|^2 + |C^-|^2)C^+\right. \\
&\quad \left. + (1-\alpha)\frac{\partial}{\partial t}(\mathrm{Re}(C^+C^{-*}))C^-\right]; \\
\frac{\partial C^-}{\partial z} &= +\frac{\Delta\beta_1}{2}\frac{\partial C^-}{\partial t} - \mathrm{j}\frac{\beta_2}{2}\frac{\partial^2 C^-}{\partial t^2} + \frac{\beta_3}{6}\frac{\partial^3 C^-}{\partial t^3} \\
&\quad + \frac{g}{2}C^- + \frac{1}{L_\mathrm{a}\Omega_\mathrm{a}^2}\frac{\partial^2 C^-}{\partial t^2} \\
&\quad + \frac{2\mathrm{j}\gamma}{3}(|C^-|^2 + 2|C^+|^2)C^- \\
&\quad - \mathrm{j}\gamma T_\mathrm{R}\left[\frac{1+\alpha}{2}\frac{\partial}{\partial t}(|C^+|^2 + |C^-|^2)C^-\right. \\
&\quad \left. + (1-\alpha)\frac{\partial}{\partial t}(\mathrm{Re}(C^+C^{-*}))C^+\right].
\end{aligned} \tag{1}$$

The first right-hand terms in equation (1) account for the group velocity mismatch between circular polarization components ($\Delta\beta_1 = \beta_1^+ - \beta_1^- = 1/v_\mathrm{g}^+ - 1/v_\mathrm{g}^-$ is the inverse group velocity mismatch caused by twist [43]), the second and third terms describe dispersion (β_2 and β_3 are the second- and third-order dispersion parameters, respectively), the fourth and fifth terms account for gain and gain dispersion, respectively (g is gain per unit length, L_a is the doped fibre length and Ω_a the gain bandwidth in Hz), and are included only for integration over the amplifier section. The following terms are Kerr nonlinear terms of self- and cross-phase modulation, where γ is the Kerr nonlinear coefficient, and finally the last terms take into account the Raman self-frequency shift [44]. $T_\mathrm{R} = 3$ fs is the Raman delay and $\alpha = 0.3$ is the cross-polarization Raman coefficient at low frequency shift [45]. Time t is referenced in a system that travels at the average group velocity $v_\mathrm{g} = 2/(\beta_1^+ + \beta_1^-)$. The gain is considered uniform across the amplifier section, and saturates on the pulse energy E_p through

$$g = \frac{g_0}{1 + E_\mathrm{p}/E_\mathrm{sat}}, \tag{2}$$

where E_sat is the saturation energy. A value of unsaturated gain of $g_0 = 1.66\ \mathrm{m}^{-1}$ is sufficient to ensure signal growth at low intracavity power. The saturation energy is set to a value for which the temporal extension of the pulses is limited to ~100 ps, in order to keep computational time within reasonable limits. Finally, a 3 dB gain bandwidth of 80 nm is considered.

Because multiple pulsing was observed experimentally to originate from the splitting of a long, low-peak-power single noise-like pulse when the NOLM switching power is low, we considered in this study the case of minimal NOLM switching power, by setting the angle of the polarizer at the NOLM input to 45° with respect to the QWR axes [41, 42]. For the parameters used in this simulation, the minimal NOLM switching power is ~250 W. Taking a small-amplitude Gaussian noise as the initial signal, integration is performed over successive cycles using a split-step Fourier algorithm, until convergence is reached.

This study did not allow us to observe any case of stable multiple noise-like pulsing in the regime. In practically all of our simulations, a stable, single noise-like pulse finally emerges. Although the details of the waveform vary after successive round-trips, the global pulse characteristics (average peak power, total duration, optical bandwidth) remain stable. Figure 5(a) shows a superposition of successive waveforms at the NOLM output in the regime. The roughly rectangular envelope of the pulses and an average peak power of ~200–300 W confirms the idea of peak power clamping to the NOLM switching power. The typical double-scaled autocorrelation trace and the wide and smooth average spectrum observed experimentally are also consistently reproduced by the numerical study. Similar results have been obtained and discussed previously in [28]. Although multiple pulsing was not observed in the regime, in a few cases a transitory situation occurs in which two noise-like pulses coexist in the cavity. At some stage the power levels of the two noise-like pulses are similar, however one of them then tends to grow at the expense of the other (figure 5(b)), until finally only one noise-like pulse remains in the regime. An interesting feature of these two pulses is that their optical spectra, although similar, are slightly shifted one with respect to the other, by a few nm (figure 5(c)). Note the spiky appearance of the spectra in figure 5(c), which were computed each from a single waveform, without any averaging.

The extreme variability of the multiple pulsing regime under small wave retarder adjustments is commonplace in fibre lasers [5–8, 17, 46, 47]. Compared with the case of identical soliton-like pulses, where it is usually safe to assume that the pulses only suffer minor changes after successive round-trips, in the case of noise-like pulses the analysis is complicated by the fact that the inner sub-pulses suffer drastic variations within each round-trip in the cavity. Even so, parallels can be drawn with the case of multisoliton generation. In particular, the noise-like pulse breaking observed in figure 2(c) can be compared to the breaking of a bunch of identical solitons, in which a repulsive interaction mediated by dispersive waves or wavelength-shifted CW components causes the pulses to move apart from each other [5, 8, 10]. Indeed, it was shown that the interaction of pulses with dispersive waves or CW components results in small shifts in the central wavelength of the individual pulses [5, 48, 49]. The magnitude of these changes and their

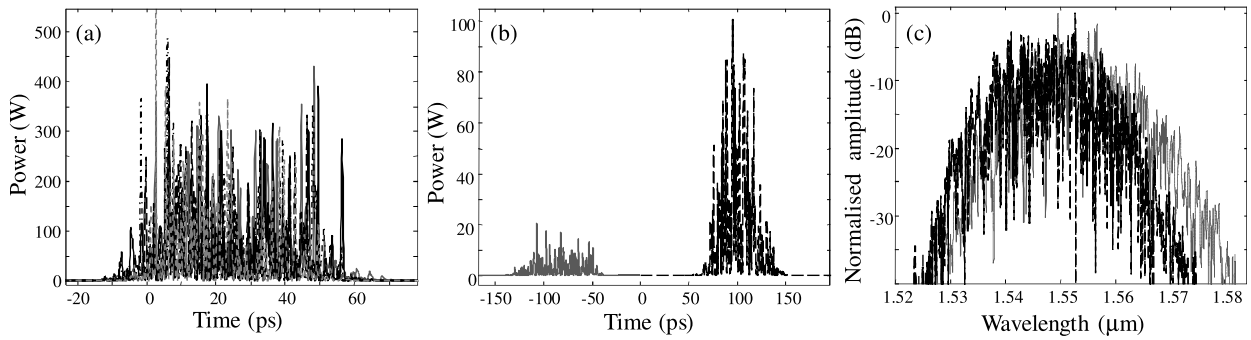

Figure 5. Simulation results. (a) Waveforms at the NOLM output in the regime after successive round-trips; (b) a transitory dual-pulse waveform (at the NOLM input); (c) optical spectra of the two noise-like pulses (when their amplitudes are nearly equal).

sign, which determines the type of interaction (attraction or repulsion) in the dispersive medium, depend on the phase between the solitons and the nonsoliton waves [5]. Now the phase between each soliton and these waves critically depends on wave retarder adjustments, so that for particular adjustments, the wavelength shifts cause the pulses to move apart in the dispersive cavity.

The above principle can be invoked to explain noise-like pulse splitting in the present experiment, considering that particular wave plate adjustments lead to the repulsive interaction described above; small wavelength shifts appear between different subsets of inner pulses in the bunch, which are sufficient to break the initial single noise-like pulse into multiple subsets of inner pulses. Although the interaction distance is usually limited in the case of dispersive waves due to their limited spatial extension, this limitation disappears in the case of CW-mediated interactions, so that a permanent walkoff between unsynchronized pulses is observed. The value of walkoff estimated experimentally on the scope (a few μs s^{-1}) together with the value of cavity dispersion allows us to determine that the wavelength shift between noise-like pulses is relatively small, of the order of 1 nm. This value is consistent with the spectral shift obtained numerically in figure 5(c). Within each subset, the central wavelengths of the sub-pulses are less dispersed than those of the different subsets, so that their repulsive interaction is not strong enough to break the cohesion between them. Although in many measurements no CW component is observable in the spectrum, background noise is clearly visible on the scope traces in figures 2(d) and (e) [6]. Besides, it was shown numerically that even a very weak CW signal (at a level down to -10^{-5} times smaller than the pulse peak intensity) has a substantial effect [49], so that we believe that this mechanism plays an important role in the onset of multiple pulsing in our scheme.

Once unsynchronized noise-like pulses circulate in the cavity, slight adjustments of the wave retarders allow us to eliminate (or balance) the long-range interactions, yielding stable multiple pulsing. The constant, 20 ns separation between various consecutive pulses observed in figures 2(d) and (e) may be the signature of a remaining repulsive interaction mediated by the dispersive waves, the 20 ns upper limit of the interaction range then being the duration of these dispersive components accompanying the pulses. In this case, the patterns of figures 2(d) and (e) can be interpreted as regular though incomplete pulse trains, presenting a constant 20 ns period but in which a large number of pulses are lacking. This suggests that, at substantially higher pump power, the empty intervals would be filled with additional pulses, leading to high-order harmonic mode locking of noise-like pulses.

Another point deserving attention is the fact that multiple noise-like pulses are systematically observed at the low-peak-power, long-duration limit of single pulsing. First, it seems reasonable to state that the longest noise-like pulse, which contains the largest number of sub-pulses (several tens of thousands), is the most likely to become unstable and split, for example under the effect of some perturbation. Secondly, assuming that the cohesion between sub-pulses in a noise-like pulse is of the same nature as the direct soliton–soliton interaction in bound structures, the binding energy between these sub-pulses is proportional to the sub-pulse energy [9]. Hence, when the noise-like pulse has a low-peak-power value, and thus the sub-pulses have low energies, the cohesion between them is reduced and can be easily overcome by the repulsive interaction mediated by dispersive or CW components, so that the noise-like pulse splits into a few subsets of pulses. If now the NOLM switching power is further reduced, the cohesion between the inner pulses is weakened further so that these subsets split again, until a maximum number of 12 noise-like pulses coexist in the cavity. Finally, it has to be observed that when multiple pulsing takes place, the optical spectrum is the narrowest (4.5 nm for the dotted line in figure 3(c), compared with ~50 nm for the gain bandwidth). There is thus a high level of gain available for wavelength-shifted components, which are then able to maintain themselves in the cavity. The inhomogeneous broadening of the gain medium may also be helpful to mitigate gain competition and allow the coexistence of spectrally shifted components.

As pointed out earlier, our numerical results confirm the possibility of splitting of a single noise-like pulse. It is also significant that the two resulting noise-like pulses are slightly shifted spectrally, as such small spectral shifts are consistent with the long-distance pulse interaction mechanisms discussed above. As no CW component is visible outside the pulses (figure 5(b)), the wavelength shift

is possibly caused by dispersive waves accompanying the pulses. On the other hand, the absence of multiple pulsing in the regime in the numerical study contrasts with the experimental results. It can be related to the limited duration of the noise-like pulse allowed in the simulations, which for the sake of saving computational time was maintained at values more than two orders of magnitude below the single-pulse duration observed experimentally just before splitting. Besides, inhomogeneous broadening, which is believed to play a role in mitigating the gain competition between noise-like pulses, was not included in the model.

The pattern observed in figure 4(b) strongly recalls bound states of multiple solitons (see figure 4 in [50]), suggesting some kind of analogy, however the different timescale (larger by three orders of magnitude), the autocorrelation trace and the optical spectrum associated with the present regime clearly indicate the noise-like nature of the structure. Although the discussion presented above does not allow us to elucidate this peculiar regime, it is useful to improve our understanding of the processes leading to multiple noise-like pulsing in fibre lasers.

5. Conclusions

In summary, we demonstrated experimentally multiple noise-like pulsing in a long erbium-doped figure-eight fibre laser in the normal net dispersion regime. The laser includes a polarization-imbalanced NOLM as the saturable absorber. Polarization control at the NOLM input allows us to adjust the NOLM switching power. For proper adjustments, mode locking is obtained and a stable noise-like pulse builds up in the cavity, the peak power of which appears to be clamped to the NOLM switching power. If this power is reduced through polarization control, the duration of the noise-like pulse grows correspondingly and its spectral width decreases. Beyond a duration of ∼22 ns, the pulse splits into multiple noise-like pulses. Up to 12 simultaneous noise-like pulses were observed experimentally, which can be synchronized although their spacing remains irregular. Our experimental results, together with our numerical analysis, suggest that multiple pulsing originates from repulsive interaction between subsets of inner pulses in the bunch, which is mediated by the dispersive wave and CW components accompanying the pulses. When the NOLM switching power is adjusted to a low value so as to form a long, low-peak-power noise-like pulse in which the cohesion between inner pulses is weakened, this pulse tends to split into multiple noise-like pulses under the action of such repulsive forces. Hence, controlling the NOLM switching power allows us to determine indirectly the single or multiple noise-like pulse operation of the laser. Although the multiple pulse patterns are unstable, synchronization is obtained once the long-range interaction is cancelled through small wave retarder adjustments. For applications, the generation of a single pulse with high energy and broad bandwidth is highly desirable, so that the saturable absorber has to be carefully designed and adjusted to avoid multiple pulsing. Finally, the broadband quadruple pulse regime in particular demonstrates the potential of noise-like pulses for applications such as supercontinuum generation and sensing, and exemplifies the fact that a lot of work still lies ahead to reach a full understanding of the mechanisms underlying the formation of these pulses.

Acknowledgment

O Pottiez was supported by CONACyT grant 130681.

References

[1] Kobtsev S M, Kukarin S V, Smirnov S V and Fedotov Y S 2010 *Laser Phys.* **20** 351–6
[2] Li X H, Wang Y G, Wang Y S, Zhang Y Z, Wu K, Shum P P, Yu X, Zhang Y and Wang Q J 2013 *Laser Phys. Lett.* **10** 75108
[3] Liu T, Jia D, Yang J, Chen J, Wang Z and Yang T 2013 *Laser Phys.* **23** 95005
[4] Grudinin A B, Richardson D J and Payne D N 1992 *Electron. Lett.* **28** 67
[5] Grudinin A B and Gray S 1997 *J. Opt. Soc. Am.* B **14** 144–54
[6] Tang D Y, Zhao B, Zhao L M and Tam H Y 2005 *Phys. Rev.* E **72** 16616
[7] Amrani F, Haboucha A, Salhi M, Leblond H, Komarov A and Sanchez F 2010 *Appl. Phys.* B **99** 107–14
[8] Zhang Z X, Zhan L, Yang X X, Luo S Y and Xia Y X 2007 *Laser Phys. Lett.* **4** 592–6
[9] Komarov A, Haboucha A and Sanchez F 2008 *Opt. Lett.* **33** 2254–6
[10] Amrani F, Haboucha A, Salhi M, Leblond H, Komarov A, Grelu Ph and Sanchez F 2009 *Opt. Lett.* **34** 2120–2
[11] Sobon G, Krzempek K, Kaczmarek P, Abramski K M and Nikodem M 2011 *Opt. Commun.* **284** 4203–6
[12] Renninger W H, Chong A and Wise F W 2008 *Opt. Lett.* **33** 3025–7
[13] Pottiez O, Ibarra-Escamilla B, Kuzin E A, Grajales-Coutiño R and Carrillo-Delgado C M 2010 *Laser Phys.* **20** 709–15
[14] Erkintalo M, Aguergaray C, Runge A and Broderick N G R 2012 *Opt. Express* **20** 22669–74
[15] Lin J-H, Jhu J-L, Jyu S-S, Lin T-C and Lai Y 2013 *Laser Phys.* **23** 25103
[16] Komarov A, Amrani F, Dmitriev A, Komarov K and Sanchez F 2013 *Phys. Rev.* A **87** 23838
[17] Grelu Ph and Soto-Crespo J M 2004 *J. Opt. B: Quantum Semiclass. Opt.* **6** S271–8
[18] Peng J, Zhan L, Luo S and Shen Q S 2013 *IEEE Photon. Technol. Lett.* **25** 948–51
[19] Tang D Y, Zhao L M, Zhao B and Liu A Q 2005 *Phys. Rev.* A **72** 43816
[20] Kärtner F X, Aus der Au J and Keller U 1998 *IEEE J. Sel. Top. Quantum Electron.* **4** 159–68
[21] Lederer M J, Luther-Davies B, Tan H H, Jagadish C, Akhmediev N N and Soto-Crespo J M 1999 *J. Opt. Soc. Am.* B **16** 895–904
[22] Horowitz M, Barad Y and Silberberg Y 1997 *Opt. Lett.* **22** 799–801
[23] Horowitz M and Silberberg Y 1998 *IEEE Photon. Technol. Lett.* **10** 1389–91
[24] Kang J U 2000 *Opt. Commun.* **182** 433–6
[25] Takushima Y, Yasunaka K, Ozeki Y and Kikuchi K 2005 *Electron. Lett.* **41** 399–400
[26] Tang D Y, Zhao L M and Zhao B 2005 *Opt. Express* **13** 2289–94
[27] Zhao L M and Tang D Y 2006 *Appl. Phys.* B **83** 553–7
[28] Pottiez O, Grajales-Coutiño R, Ibarra Escamilla B, Kuzin E A and Hernandez-Garcia J C 2011 *Appl. Opt.* **50** E24–31

[29] Vazquez-Zuniga L A and Jeong Y 2012 *IEEE Photon. Technol. Lett.* **24** 1549–51
[30] Pottiez O, Martinez-Rios A, Monzon-Hernandez D, Salceda-Delgado G, Hernandez-Garcia J C, Ibarra-Escamilla B and Kuzin E A 2013 *Laser Phys.* **23** 035103
[31] Zhao L M, Tang D Y and Wu J 2007 *Opt. Express* **15** 2145–50
[32] Kobtsev S, Kukarin S, Smirnov S, Turitsyn S and Latkin A 2009 *Opt. Express* **17** 20707–13
[33] Zaitsev A K, Lin C H, You Y J, Tsai F H, Wang C L and Pan C L 2013 *Laser Phys. Lett.* **10** 45104
[34] Dennis M L, Putnam M A, Kang J U, Tsai T-E, Duling I N III and Friebele E J 1997 *Opt. Lett.* **22** 1362–4
[35] Hernandez-Garcia J C, Pottiez O and Estudillo-Ayala J M 2012 *Laser Phys.* **22** 221–6
[36] Duling I N III 1991 *Opt. Lett.* **16** 539–41
[37] Doran N J and Wood D 1988 *Opt. Lett.* **13** 56–8
[38] Fermann M E, Haberl F and Hofer M 1990 *Opt. Lett.* **15** 752–4
[39] Kuzin E A, Korneev N, Haus J W and Ibarra-Escamilla B 2001 *J. Opt. Soc. Am.* B **18** 919–25
[40] Tanemura T and Kikuchi K 2006 *J. Lightwave Technol.* **24** 4108–19
[41] Pottiez O, Kuzin E A, Ibarra-Escamilla B and Mendez-Martinez F 2005 *Opt. Commun.* **254** 152–67
[42] Ibarra-Escamilla B, Kuzin E A, Zaca-Moran P, Grajales-Coutiño R, Mendez-Martinez F, Pottiez O, Rojas-Laguna R and Haus J W 2005 *Opt. Express* **13** 10760–7
[43] Barlow A J and Payne D N 1983 *IEEE J. Quantum Electron.* **19** 834–9
[44] Korneev N, Kuzin E A, Villagomez-Bernabe B A, Pottiez O, Ibarra-Escamilla B, González-García A and Durán-Sánchez M 2012 *Opt. Express* **20** 24288–94
[45] Mandelbaum I, Bolshtyansky M, Heinz T F and Walker A R H 2006 *J. Opt. Soc. Am.* B **23** 621–7
[46] Chouli S and Grelu P 2009 *Opt. Express* **17** 11776–81
[47] Haboucha A, Leblond H, Salhi M, Komarov A and Sanchez F 2008 *Phys. Rev.* A **78** 43806
[48] Loh W H, Grudinin A B, Afanasjev V V and Payne D N 1994 *Opt. Lett.* **19** 698–700
[49] Komarov A, Komarov K, Leblond H and Sanchez F 2007 *J. Opt. A: Pure Appl. Opt.* **9** 1149–56
[50] Akhmediev N N, Ankiewicz A and Soto-Crespo J M 1997 *Phys. Rev. Lett.* **79** 4047–51